

RETRIEVAL OF THE TROPICAL DIVERGENT WIND FROM OLR AND ITS APPLICATION IN ENSO DIAGNOSIS*

ZHANG Yongsheng (张永生)**

LASG, Institute of Atmospheric Physics, Chinese Academy of Sciences, Beijing 100029

and JIANG Shangcheng (蒋尚城)

LSSR, Department of Geophysics, Peking University, Beijing 100871; E-mail: scjiang @ pku. edu. cn

Received April 12, 1999; revised November 4, 1999

ABSTRACT

In this paper, two schemes proposed by Julian (1984) and Krishnamauti (1986) are used to retrieve the tropical divergent wind at 200 hPa and 850 hPa from the satellite observational Outgoing Long-wave Radiation (OLR). The comparison study has been conducted among the OLR-derived divergent wind field and those directly from wind fields of ECMWF and CAC tropical analysis, and NCEP/NCAR reanalysis for examining their reliability. Then, the divergent wind retrieved from OLR by using Julian's scheme is used to composite the diagrams of the Walker circulation and the local Hadley circulation during 1982–1983 ENSO event. The possible linkage between the anomalies of summer rainfall in East China during this period and the anomalous Walker and local Hadley circulations is discussed.

It is shown that it is practically feasible to use the satellite observed OLR data in the estimation of the tropical divergent wind. It is also indicated that NCEP/NCAR reanalysis has made a progress for improving the reliability of the tropical divergent wind, though some biases still exist in the description of the intensity and position of the divergence (convergence) maximum centers over Asian monsoon region. The application of Julian's method to a diagnosis on the evolutions of the anomalous Walker and Hadley circulations during 1982–1983 ENSO event shows that the development of this ENSO event is not accompanied with the sudden reversal of the Walker circulation, but the propagation of the ascending branch over the western Pacific to the central-eastern Pacific and crossing through the date line, which results in a significant displacement of the vertical circulation over the West Pacific (WP) and the central-east Pacific (CEP). It is also indicated that there exists a close linkage between the change of local Hadley circulation in the WP and the Walker circulation in the CEP, implying that the Walker circulation possibly serves as a bridge between the anomalies of the SST in the CEP and the change of local Hadley circulation in Northwest Pacific. The latter is responsible for the climate anomaly over eastern China during this period.

* This research is supported by the Chinese Ninth Five-Year National Project "Short-Range Climate Prediction System" and the National Natural Science Foundation of China project for the young scientists, Grant No. 49705061.

** Corresponding author address: Dr. ZHANG Yongsheng, International Pacific Research Center, SOEST, University of Hawaii, 2525 Correa Road, Honolulu, HI 96822, USA; E-mail: yzhang @ soest. hawaii. edu

Key words: OLR (Outgoing Long-wave Radiation), divergence, Walker circulation, Hadley circulation, ENSO

1. INTRODUCTION

The Outgoing Long-wave Radiation (OLR) measured by the satellite is an important component in the budget of earth radiation. In the tropical region, it provides not only the information on the distribution and the variability of the atmospheric heating sources and sinks, but also the information on the activities of the tropical convection, air-sea interaction, precipitation, and divergent wind field. Therefore, the satellite observational OLR data have been used widely in the tropical weather and climate study during recent years (Jiang and Zhu 1990).

Because the conventional meteorological observations in the vast tropics are rarer than those in the extratropical latitudes, it is difficult to obtain a desirably accurate description of the divergent wind in the tropics if only depending on the conventional observations. The observational studies have revealed that there exist very strong convective activities and relatively strong ageostrophic circulation in the tropics with the divergent component of the wind being equal to or even dominant over the rotational component. Therefore, it is necessary to use other non-conventionally observational data to supplement the conventional data in order to improve the quality of the analysis of divergent wind in the tropics.

In the vast tropics, considering that the sea surface temperature (SST) displays a relatively small temporal and spatial variability, the OLR is mainly decided by the cloud quantity and the temperature at the top of cloud. The latter, to some degree, indicates the intensity of the tropical convection: strong convection corresponds to high cloud top with low temperature and thus corresponds to low OLR values; weak convection corresponds to low cloud top with high temperature and thus corresponds to high OLR values. In the strong convection areas, the ascending motion dominates with divergence at upper troposphere and convergence at lower troposphere. In the subsidence areas, the descending motion dominates with convergence at upper troposphere and divergence at lower troposphere. So OLR is positively correlated with the upper-level divergence and negatively correlated with the lower-level divergence. OLR is also negatively correlated with the vertical velocity at non-divergence level. Therefore, it is physically possible to retrieve the divergent wind field from the satellite OLR data over the tropics.

Julian (1984) proposed a scheme in which the tropical divergent wind field is calculated from OLR data. According to the scheme, the tropical wind field is divided into the rotational and divergent components. The OLR data, expressed in equivalent blackbody temperature (TBB), are transformed firstly to divergence at various levels over the local grid, and then the velocity potential field is calculated from the divergence field. Subsequently, the divergent wind field is obtained from the velocity potential. Table 1 given by Julian (1984), shows the OLR (in TBB) conversion to divergence. This table has been obtained after examining a large quantity of the divergence, vorticity, vertical velocity, precipitation, radar and satellite data in the tropics. In order to verify its

reliability. Julian (1984) selected a lot of cases during the first GARP (Global Atmospheric Research Program) global experiment (FGGE) period and compared the OLR-derived divergent wind with that of being obtained by the ECMWF assimilation data. He found that over the tropics where the conventional observation data are sparse, the quality of the OLR-derived divergent wind field is superior to that of being obtained from ECMWF analysis data.

Table 1. Conversion of TBB (K) to Divergence (10^{-6} s^{-1}) Proposed by Julian (1984)

TBB (K)	hPa											
	150	200	250	300	400	500	600	700	800	850	900	950
210	40	29	20	8	0	-2	-4	-6	-10	-12	-15	-22
215	38	30	22	10	0	-2	-4	-6	-12	-14	-17	-22
220	30	40	28	14	0	-2	-3	-5	-13	-18	-20	-23
225	23	35	40	16	2	0	-2	-5	-16	-21	-25	-26
230	20	22	29	20	8	0	-1	-4	-12	-20	-24	-25
235	40	14	18	13	6	0	-1	-2	-8	-10	-14	-16
240	3	7	10	8	5	0	0	-1	-3	-7	-8	-10
245	1	4	4	3	3	0	0	-1	-1	-3	-4	-5
250	0	3	3	0	0	0	0	0	0	0	0	-3
255	0	0	0	0	0	0	0	0	0	0	0	0
260	-2	-2	-1	0	0	0	0	0	0	0	1	2
265	-4	-3	-1	0	0	0	0	0	0	0	2	3
270	-8	-7	-4	-1	0	0	0	1	2	2	3	5
275	-14	-12	-6	-2	0	0	0	2	4	5	6	8
280	-18	-15	-8	-2	0	0	0	4	5	6	8	9

Krishnamauti (1986) proposed a scheme from a statistical regression between the divergence at 200 hPa field and OLR at individual grid in the tropics. In his work, 35 cases were selected during FGGE period, in which the divergence fields were calculated from ECMWF data. For exploring a good statistical relationship between OLR and the divergent field at different horizontal resolutions, the expansions of the spherical harmonic for divergence and OLR were performed. A regression analysis among wind divergence ($\nabla^2\chi$), OLR and ∇^2R (R indicates OLR) was carried out at different zonal wave number $J=1, 2, 3, \dots, 12$. The results show that the maximum value of 0.76 for the correlation is obtained at a resolution of $J=8$. The regression equation at this resolution is expressed by

$$D = -\nabla^2\chi = 0.2814 \times 10^{-7}R - 0.2036 \times 10^5 \nabla^2R - 0.7069 \times 10^{-5},$$

where the unit of the OLR (R) is W m^{-2} and the unit of divergence is s^{-1} . This formula indicates that the upper-level (200 hPa) divergence (convergence) corresponds to lower (higher) OLR values. This formula is confined to the large-scale analysis within $30^\circ\text{S} - 30^\circ\text{N}$.

In recent years, some relevant work has been done by a lot of Chinese researchers. Xie and Bai (1993) applied Julian scheme to more cases. Their purpose has been to explore the possibility of improving the analysis of the divergent wind by using OLR and to find

some practical ways involving in how to introduce the OLR data in the operational numerical prediction.

In this paper, our efforts will be put into further verifying and improving the retrieval methods and applying these methods into the diagnosis of general circulation in the tropics. Three methods are used to calculate the tropical divergent wind. The first and second methods are based on the Julian (1984) and Krishnamauti (1986) schemes, respectively, in which the divergent wind field is calculated from the satellite observational OLR. The third method directly calculates the divergent wind from the conventional analysis data. Comparisons are performed among the results from three different methods, and the detailed discussions are made on the feasibility and reliability of these methods in Sections III and IV. Based on the above experiments, these methods are used to diagnose the evolution and the anomaly of the tropical general circulation during the 1982–1983 ENSO event in Section V. The results are compared with those obtained by other data sources, and finally we will discuss the impact of ENSO on the circulation anomalies over the Pacific Ocean which cause the anomaly of the summer rainfall over Changjiang (Yangtze) River Valley in China.

II. DATA AND METHODS

1. Data

The OLR data observed from the satellites of NOAA series used in our research include the daily and monthly mean (0000 UTC and 1200 UTC, twice daily) with a horizontal resolution of 2.5° latitude by 2.5° longitude. The detailed description of the data can be seen in the literature of Jiang and Zhu (1990).

The wind data are from ECMWF objective analysis at 1200 UTC archived in a resolution of 2.5° latitude by 2.5° longitude and the U. S. CAC/NMC (formerly NCEP) monthly tropical analysis archived in about 5° latitude-longitude blocks. Additionally, an updated wind data from NCEP/NCAR reanalysis are used in our work with the same time interval and spatial grid of OLR.

2. Methods

In the present paper, three different schemes are used to calculate the divergence, velocity potential and divergent wind field.

Scheme 1: called K-scheme for short, which is based on the statistically regressed relation proposed by Krishnamauti (1986):

$$D = -\nabla^2\chi = 0.2814 \times 10^{-7}R - 0.2036 \times 10^5 \nabla^2 R - 0.7069 \times 10^{-5}, \quad (1)$$

where R is the OLR value, in W m^{-2} , D the divergence at 200 hPa, in s^{-1} , χ the velocity potential in $\text{m}^2 \text{s}^{-1}$.

After the divergence field is obtained, iterative method is used to solve the equation

$$D = -\nabla^2\chi. \quad (2)$$

If the velocity potential χ is obtained, then the divergent wind is calculated with the following formula

$$U_x = - \frac{\partial \chi}{a \cos \varphi \partial \lambda}, \quad (3)$$

$$V_x = - \frac{\partial \chi}{a \partial \varphi}, \quad (4)$$

where a , φ and λ are radius of the earth, latitude and longitude, respectively. It is seen from (2) that the high velocity potential value center corresponds to divergent area and the low velocity potential center corresponds to convergent area. The divergent wind, according to (3) and (4), blows from high value center to low value center.

Scheme 2: called J-scheme for short, which is based on the scheme proposed by Julian (1984). The conversion between the OLR (in TBB temperature) and the divergence at various levels over the same horizontal grid is listed in Table 1. After getting the divergence field from the OLR data based on Table 1, the velocity potential field is obtained by solving Eq. (2) iteratively. Then the divergent wind field is calculated with Formulas (3) and (4).

Scheme 3: called direct scheme. That is, the ECMWF, CAC and NCEP/NCAR reanalysis wind data are used directly to calculate the divergence:

$$D = \frac{\partial u}{\partial x} + \frac{\partial v}{\partial y}. \quad (5)$$

Then, Formulas (2), (3) and (4) are used to calculate the velocity potential and the divergent wind.

It is worth being pointed out that no matter which scheme is used, the difference among them lies in the different ways to get divergence field. After that, same Formulas (2), (3) and (4) are used to calculate the velocity potential and divergent wind, which leads to the comparability of results among the three schemes.

3. Retrieval of the Tropical Zonal and Meridional Vertical Circulation

Using Julian's scheme (scheme 2), the divergent winds U_x and V_x at 850 hPa and 200 hPa are calculated from OLR data. Then the divergences of the zonal and meridional winds are obtained from the following formulas:

$$D_u = \frac{\partial U_x}{\partial x} = - \frac{\partial^2 \chi}{a^2 \cos^2 \varphi \partial \lambda^2}, \quad (6)$$

$$D_v = \frac{\partial V_x}{\partial y} = - \frac{\partial^2 \chi}{a^2 \partial \varphi^2}. \quad (7)$$

By use of continuity equation

$$\frac{\partial u}{\partial x} + \frac{\partial v}{\partial y} + \frac{\partial \omega}{\partial p} = 0, \quad (8)$$

or

$$D + \frac{\partial \omega}{\partial p} = 0,$$

we have

$$\omega = \int_{p_1}^{p_2} D dp. \quad (9)$$

The difference of the divergence between 200 hPa and 850 hPa is used as the characteristic index to represent the vertical circulation. We further define the index of the

mean zonal (meridional) vertical circulation between two latitudes (longitudes) Y_1 and Y_2 (X_1 and X_2):

$$I_w(\lambda) = -\frac{1}{Y_2 - Y_1} \int_{Y_1}^{Y_2} (D_{u200} - D_{u850}) dy, \quad (10)$$

$$I_H(\varphi) = -\frac{1}{X_2 - X_1} \int_{X_1}^{X_2} (D_{v200} - D_{v850}) dx. \quad (11)$$

In the present paper, Y_1 and Y_2 are assigned 10°S and 10°N . X_1 and X_2 are assigned 110°E and 160°E . $I_w(\lambda)$ represents the index of the Walker circulation and $I_H(\varphi)$ represents the index of the local Hadley circulation over the West Pacific Ocean. With I_w , I_H , U_x and V_x , we can roughly define the diagram of the Walker circulation and the Hadley circulation from the satellite OLR data.

It should be pointed out that we are only able to obtain the divergence directly from OLR data, so in order to separate the circulation components, we have to solve the velocity potential, and then calculate the divergent wind, D_u and D_v . If we use the conventional wind-observational data, the D_u and D_v can be directly calculated.

III. COMPARISON OF OLR-DERIVED VELOCITY POTENTIAL AND DIVERGENT WIND WITH ECMWF ANALYSIS AND CAC TROPICAL ANALYSIS

Using the above-mentioned three schemes, we calculated the daily, 5-day, 10-day and monthly mean divergences, velocity potentials and divergent winds. Among the large numbers of the cases, some of them were selected for comparing the differences of the results in the three schemes. Our attention is focused on the areas where the large differences exist and to discuss the possible causes in order to demonstrate the reliability in using OLR to derive divergent wind.

Figure 1 shows the January 1979 monthly mean velocity potential at 200 hPa derived from the three schemes. The range of the values is situated between $10^5 - 10^6 \text{ m}^2 \text{ s}^{-1}$. Although the result from the K-scheme (Fig. 1a) is a little less than the result from the J-scheme (Fig. 1c), the patterns from both schemes are generally similar to each other. It indicates that the two OLR-based schemes lead to similar results. Comparing the OLR-derived results (Figs. 1a, 1c) with that directly from analysis wind (Fig. 1b), it is shown that they are consistent with each other over the southern part of Africa (50°S —equator, $20 - 40^\circ\text{E}$) where a divergent center is located, and over the South America (15°S —equator, $30 - 80^\circ\text{W}$) where a convergent center is located. The major difference among them occurs around date line and over the Tibetan Plateau. The results of both J-scheme and K-scheme indicate that a maximum center of velocity potential (corresponding to a strong divergence or a strong ascending motion) is present around the west of the date line to the south of the equator, while the result from the analysis wind shows that this maximum center is located to the east of the date line, shifting 30° longitude eastward in position comparing the maximum center derived from OLR. The map of monthly OLR in January 1979 (Jiang and Zhu 1990) shows that the maximum center of velocity potential derived from the OLR for both J-scheme and K-scheme corresponds to a low value of OLR of 180 W m^{-2} , while the maximum center derived from the analysis wind corresponds to a value of 220 W m^{-2} . It is evident that the convection over the former location is much

more intense than that over the latter one. Therefore, it could be deduced that the results from the satellite OLR data are more reliable than that from the analysis wind field. The possible reason is involved that the observational data are very sparse over this region. Over the Tibetan Plateau, the results from both J-scheme and K-scheme show the presence of maximum center of velocity potential, while the result from the data of analysis wind indicates a low center. This large difference is possibly caused by the high terrain of the plateau: during the winter, the plateau is a cold source with a very low surface temperature which leads to the low value of OLR and the corresponding high value of velocity potential in K-scheme and J-scheme. Unlike over the vast oceanic area, the low

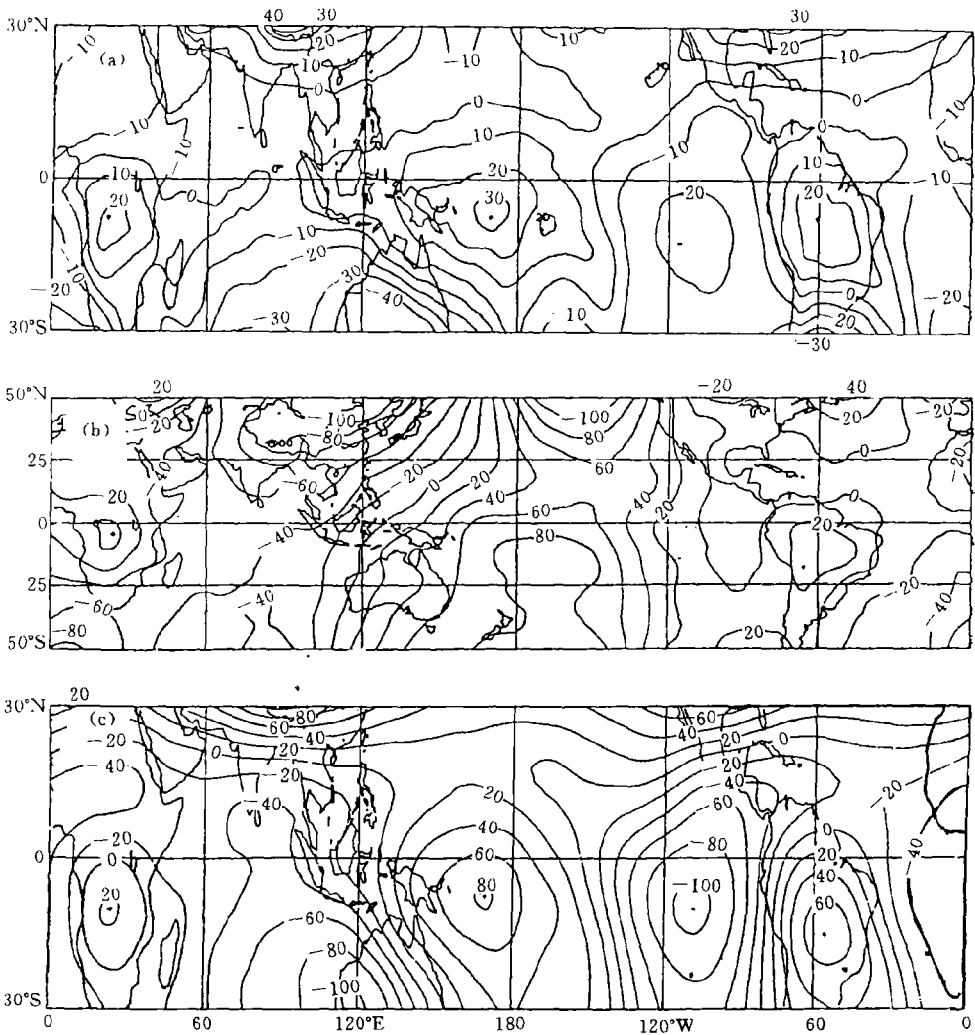


Fig. 1. The monthly mean 200 hPa velocity potential of January 1979 calculated by the three different schemes. (a) K-scheme. (b) Direct-scheme, from CAC/NMC tropical analysis wind. (c) J-scheme with contour interval (a) $1.0 \times 10^5 \text{ m}^2 \text{ s}^{-1}$; (b) and (c) $2.0 \times 10^5 \text{ m}^2 \text{ s}^{-1}$.

value of OLR does not account for the strong convection over this region. It indicates an unreliability for using OLR to derive the divergent wind field over the Tibetan Plateau.

Figure 2 shows the 5-day mean divergent wind of the first pentad of January 1983 at 200 hPa. There exists a consistency among the three schemes over the South America and the Africa where two divergent centers are located. There also exists a consistency among them over the Indonesian Kepulauan where a strong divergent center is present. However, over the West Pacific (130–160°E, 0–25°N), the results from both J-scheme and K-scheme indicate the presence of a strong convergence center, while the result from the analysis wind shows a weak divergence center over there. At 850 hPa (Fig. 3), there exist two strong convergence centers at low-level over the Indonesian Kepulauan and central Pacific, and the divergence dominates over the West Pacific. Xie and Bai (1993) found that the OLR-derived 700 hPa divergent wind is negatively correlated with the divergent wind of the ECMWF analysis. They have pointed out that the result derived from the OLR data is more reliable. From examining the OLR maps (Jiang and Zhu 1990) and the velocity potential field at low level, it could be deduced that a descending motion dominates over the West Pacific. Thus, the results from OLR data are reliable and the ECMWF wind data should be modified in divergence component.

After large numbers of the calculation experiments and case studies, we may note that over the data-sparse tropical ocean, large differences among OLR-derived divergent wind and the ECMWF and CAC/NMC analysis is most likely to occur, especially at upper level (200 hPa). Large discrepancy also occurs over the Tibetan Plateau. Besides, there is disagreement among them on the zonal variation of the divergent wind. The largest difference occurs over the Northwest Pacific to the east of Philippine, and is mainly present at 200 hPa. At lower level (850 hPa), no obvious discrepancy among them is found. We think that over this region (the Northwest Pacific), the OLR-derived divergent

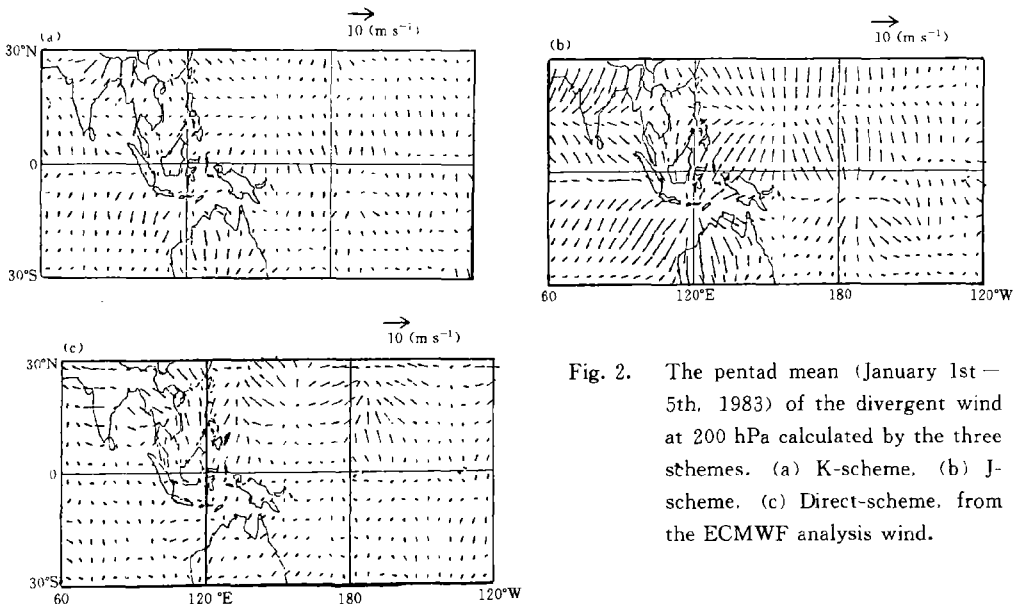


Fig. 2. The pentad mean (January 1st – 5th, 1983) of the divergent wind at 200 hPa calculated by the three schemes. (a) K-scheme. (b) J-scheme. (c) Direct-scheme, from the ECMWF analysis wind.

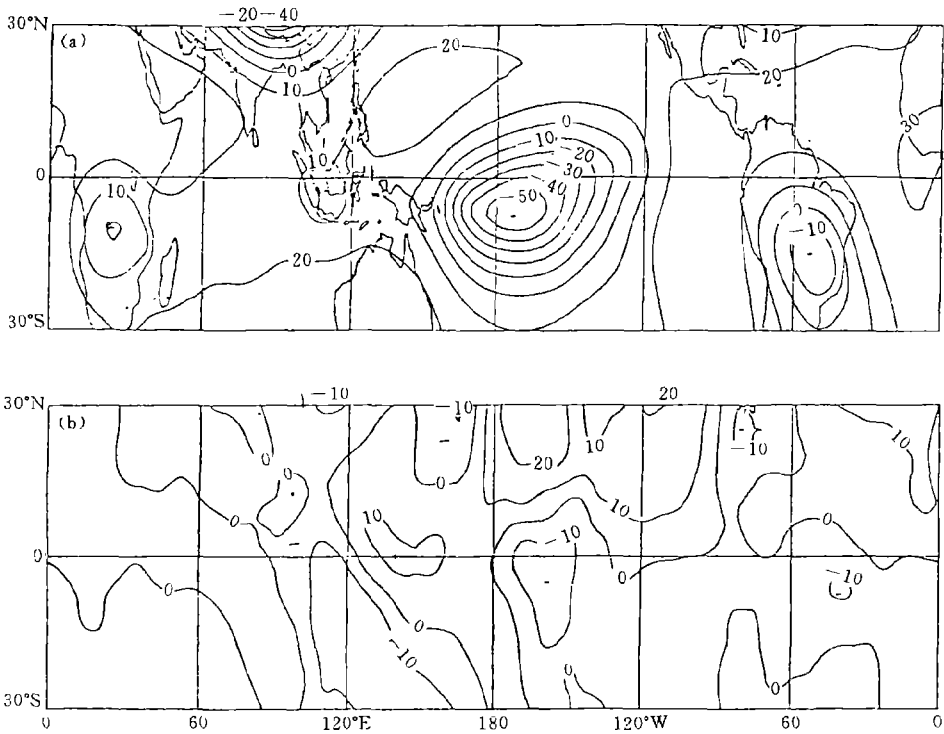


Fig. 3. The monthly mean of the velocity potential at 850 hPa in January 1983 calculated by (a) J-scheme. (b) Direct-scheme. The contour interval is $1.0 \times 10^5 \text{ m}^2 \text{ s}^{-1}$.

wind is more reliable than that of being derived from the ECMWF or CAC/NMC analysis wind. By contrast, over the Tibetan Plateau, the method for using OLR to derive divergent wind needs to be specially dealt with under a consideration of the impact of the high terrain. Over that region, the OLR value is far lower (colder) than that over the ocean areas at the same latitude. So, the J-scheme or the K-scheme can not lead to proper results. That is to imply a future work. Due to the complex information of the atmosphere contained in the OLR data, it can only be applied to the tropical region both for the schemes proposed by Julian and Krishnamauti.

IV. COMPARISON OF OLR-DERIVED DIVERGENCE WITH NCEP/NCAR REANALYSIS

During recent years, the data sets of NCEP/NCAR reanalysis have been widely used in the diagnostic study of the atmospheric circulation. How about the reliability of this new kind of data in the description of the tropical divergent wind? Some comparison and validation studies have been conducted in this section using OLR data. The monthly mean NCEP/NCAR data for the 24 months from January 1982 through December 1983 averaged from the daily (00 UTC and 12 UTC twice daily) and monthly OLR data for the same period are picked out. Then, the divergence fields are calculated by the three schemes, respectively. Our attention has been focused on the comparison of the results at 200 hPa in this section. Figure 4 shows the longitude-time cross sections of OLR and derived divergences from three schemes at 200 hPa averaged between 2.5°S — 2.5°N during 1982—

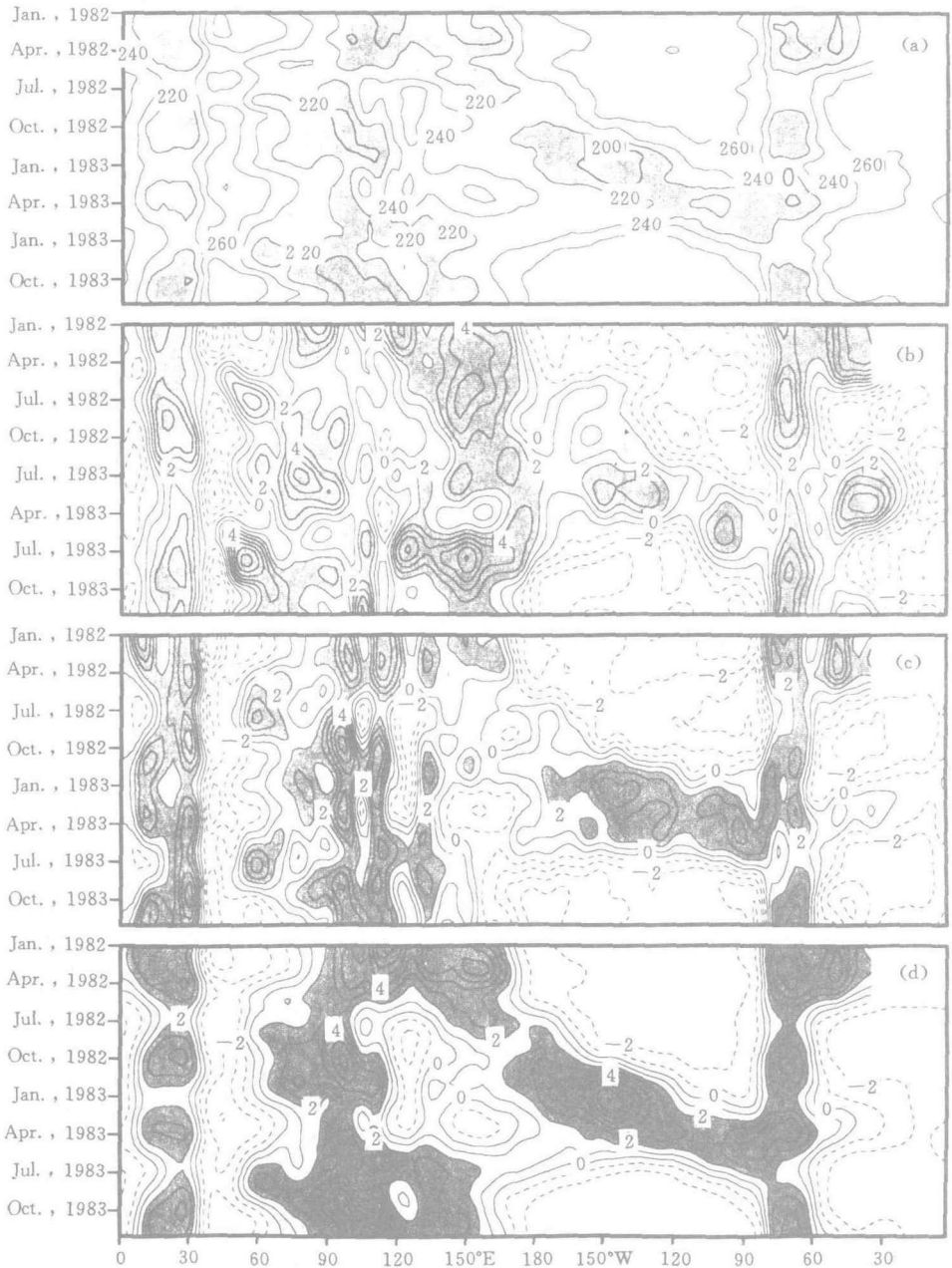


Fig. 4. The longitude-time cross sections of OLR and divergences at 200 hPa averaged between $2.5^{\circ}\text{S}-2.5^{\circ}\text{N}$ during 1982-1983. (a) OLR. Contour interval is 20 W m^{-2} with the values less than 220 W m^{-2} shaded; (b) 200 hPa divergence from NCEP/NCAR reanalysis; (c) 200 hPa divergence by K-scheme from OLR data; (d) 200 hPa divergence by J-scheme from OLR data. Contour intervals for (b), (c) and (d) are $2 \times 10^{-6} \text{ s}^{-1}$ and with values more than $2 \times 10^{-6} \text{ s}^{-1}$ shaded.

1983 (24 months). It is seen from Fig. 4a that during the 1982–1983 ENSO event, the most evident change in the tropical convection is associated with the westward shift of the strong equatorial convective center from the West Pacific to the eastern Pacific and the reversal of the strong convective activity during the winter of 1982/1983. This prominent interannual variation is captured by all the divergence fields, no matter it is calculated directly from reanalyses (Fig. 4b), or from OLR data with K-scheme (Fig. 4c) and J-scheme (Fig. 4d). They are also in good agreement concerning the position of the divergent centers around 30°E , the Indian Ocean and around 70°W . Over the West Pacific ($110\text{--}130^{\circ}\text{E}$), the result from the reanalysis (Fig. 4b) shows that a convergent center appeared during July 1982 to April 1983, while the results from OLR data (Figs. 4c, 4d) indicate that this convergence center is located $5\text{--}10^{\circ}$ further east than that from reanalyses. The latter shows that the strong divergence exists over the equatorial West Pacific, while this feature is not evident in Fig. 4c and Fig. 4d.

Therefore, Fig. 4 further demonstrates the reliability of the divergent wind from OLR data and indicates that in contrast to the earlier ECMWF analysis and CAC/NMC analysis, the NCEP/NCAR reanalysis has made much progress in the tropical divergent wind analysis.

Figures 5 and 6 present the distributions of the monthly OLR and divergence fields calculated by the three schemes at 200 hPa within the tropics (between $30^{\circ}\text{N}\text{--}30^{\circ}\text{S}$) for the January 1982 and 1983, respectively. It is seen from Fig. 5 that corresponding to the intensive convective centers, there are three strong divergence centers over the eastern Indian Ocean to the West Pacific, South America and Africa. The results from the three schemes are in good agreement concerning the description of the three divergence centers. The result from the K-scheme gives finer structures. Over the East Pacific around 5°N , the results from K-scheme and NCEP/NCAR reanalysis wind display a band-shaped divergent center, which is absent in the result from the J-scheme. The possible reason for this difference is that the divergence partly depends on the value of $\nabla^2 R$ (R represents OLR) in the K-scheme, while it depends on the relative magnitude of R in the J-scheme. It is shown in Fig. 5a that there is a relative minimum center of OLR around $180\text{--}120^{\circ}\text{W}$, $5\text{--}10^{\circ}\text{N}$, with the value ranging between 240 and 260 W m^{-2} . For the K-scheme, the value of $\partial^2 R / \partial y^2$ is relative large; while for J-scheme, 240 W m^{-2} is the critical value between the divergence and convergence. The value in the above center is larger than 240 W m^{-2} , so it is considered as a weak convergent area in J-scheme. Besides, to the north of equator ($0\text{--}10^{\circ}\text{N}$) and over the Northeast Indian Ocean, NCEP/NCAR reanalysis (Fig. 5b) shows a strong divergence, while the results from OLR data (Figs. 5c, 5d) show that the divergent center is only located over the Indian Ocean to the west of 120°E and between $0\text{--}10^{\circ}\text{S}$, and there exists a weak convergence in the Indian Ocean to the north of the equator.

Such difference between the NCEP/NCAR reanalysis and the OLR-derived divergence is also clearly shown in for the case of January 1983 (Fig. 6). It is seen from Fig. 6b that the main part of the divergence center of the eastern Indian Ocean to the West Pacific is located between $0\text{--}10^{\circ}\text{S}$, and the strong divergence is also maintained over the southern part of the South China Sea and the ocean to the southeast of Philippine, making the

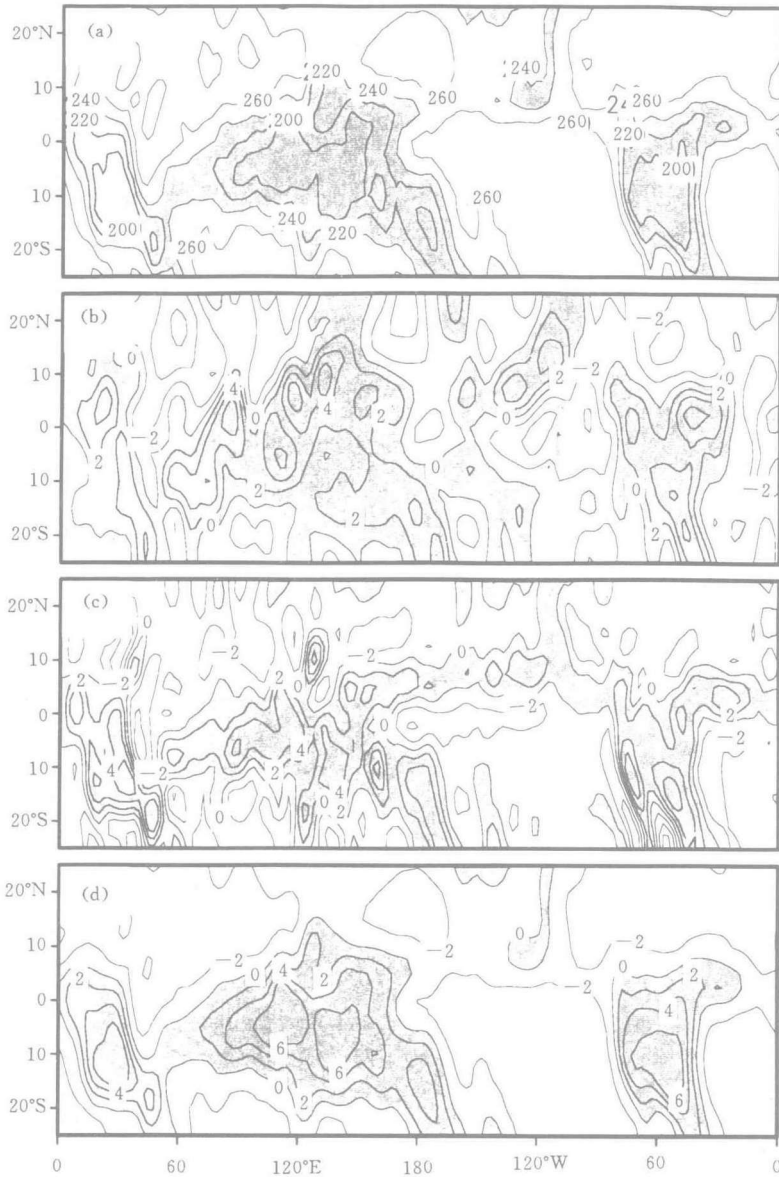


Fig. 5. The monthly mean distribution of the OLR and the divergences by the three schemes for January 1982. (a) OLR. With the contour interval of 20 W m^{-2} ; (b) 200 hPa divergence by NCEP/NCAR reanalysis; (c) 200 hPa divergence by K-scheme from OLR data; (d) 200 hPa divergence by J-scheme from OLR data. The contour interval for divergence is $2 \times 10^{-5} \text{ s}^{-1}$ with positive values shaded.

reversal of the equatorial Walker circulation not so evident during this time period. However, it is seen from Figs. 6a, 6c and 6d that during this period, the intensive convective center or the upper-level divergence center is located to the south of equator

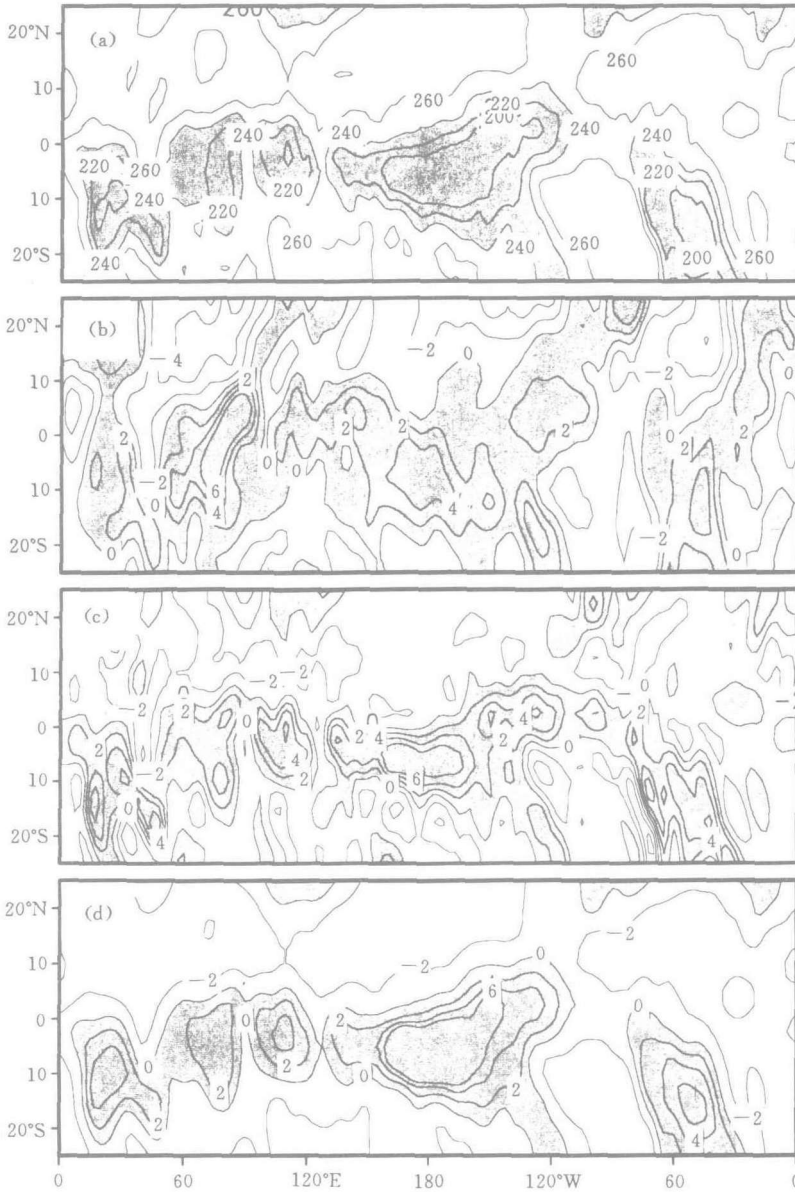


Fig. 6. As in Fig. 5, but for January 1983.

over these regions, while the strong convective center or divergence center at upper-level only presents in the eastern Pacific. Over the central Atlantic, a strong convergence center is maintained (Fig. 6b), but it is not so obvious in the OLR-derived results (Figs. 6c, 6d), indicating that the reanalysis may have a positive bias. Over these regions, since the OLR-derived divergent wind well clarifies the dominant interannual variations of the convective activities over the eastern and western Pacific during the ENSO event, the distributions of the divergent wind in NCEP/NCAR reanalysis may possibly not be proper.

In order to further examine this difference, the case of July 1983 (Fig. 7) is discussed

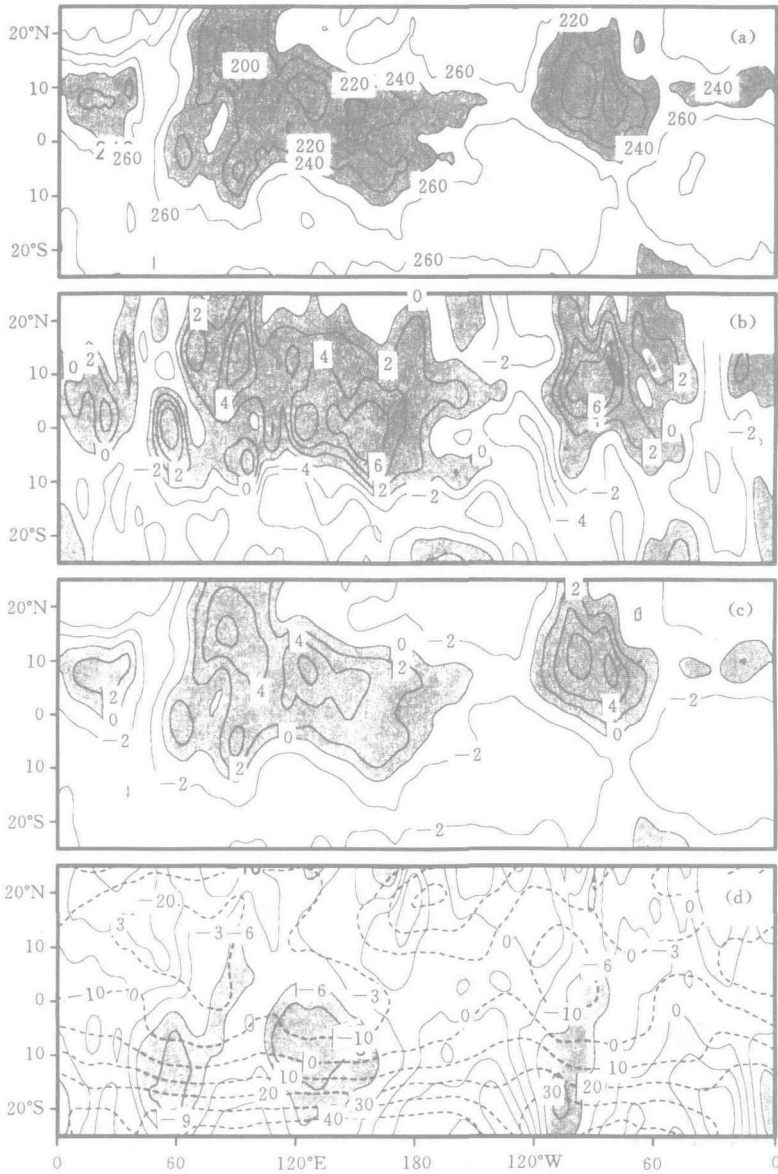


Fig. 7. The monthly mean distribution of the OLR, 200 hPa divergence and u , v for July 1983. (a), (b) and (c) as in Figs. 5a, 5b and 5d respectively, but for July 1983; (d) u and v for July 1983. Shaded areas represent $-10 \leq u \leq -5$, $-15 \leq u \leq -10$ and $u \leq -15 \text{ m s}^{-1}$ in order from light to dark, and the solid isolate is for v with the contour interval of 2 m s^{-1} and with values less than -6 m s^{-1} shaded.

then. It is seen from Fig. 7 that for the Asian monsoon region, the OLR-derived strong convergence zones are mainly located over the north of the Bay of Bengal and near Philippine (Fig. 7c, J-scheme). It well displays the seasonal variation of the tropical convective centers over the Asian monsoon region (Fig. 7a), while the NCEP/NCAR

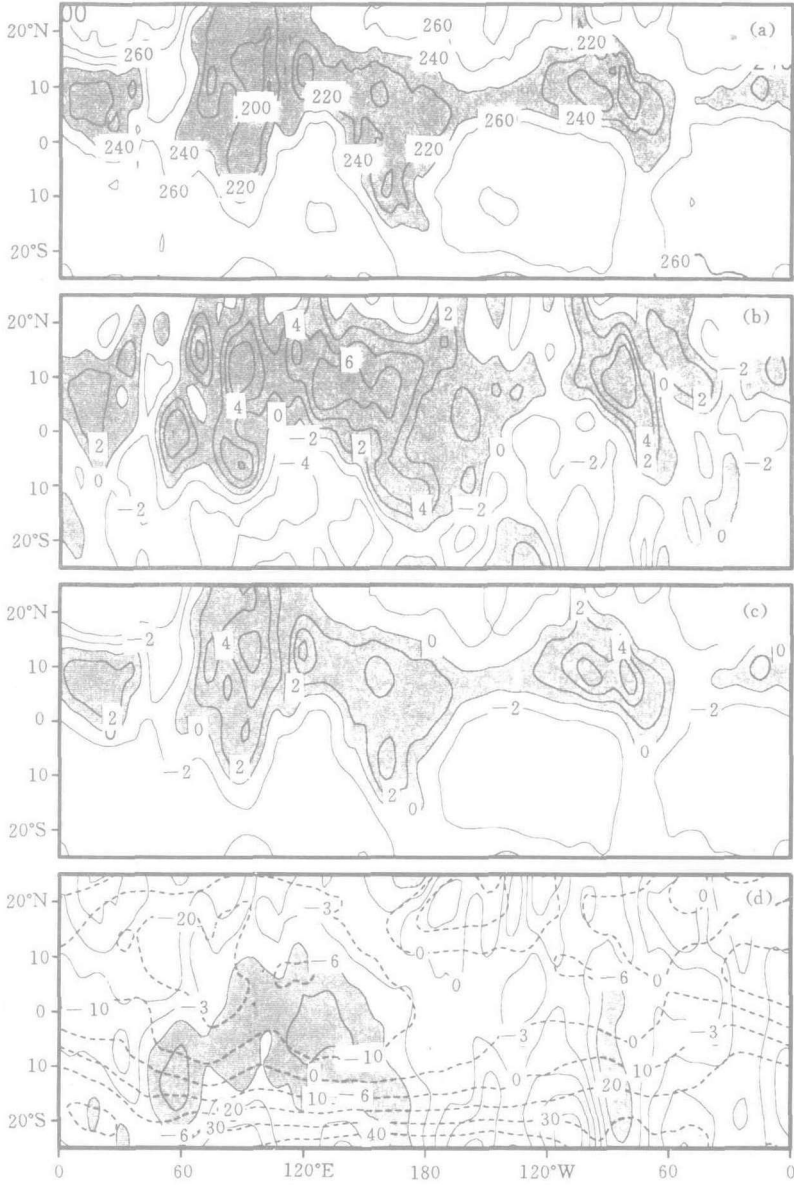


Fig. 8. As in Fig. 7. but for July 1982.

reanalysis shows an intensive convergent center near equator between 120–150°E. By contrast, for the case of July 1982 (Fig. 8), such a difference (Figs. 8b, 8c) is not evident, only the intensity of the reanalysis-derived divergence is larger than that from OLR by using J-scheme.

Webster et al. (1997) pointed out that for the majority of the numerical models, when applying in the Asian monsoon simulation, they show positive bias in the divergent field over the South Asia during the spring. According to Webster et al. (1997), such bias can be partly attributed to the complexity of the Basin of the Indian Ocean, the importance

of the land surface water cycle and the improper approximation of the Tibetan Plateau, and partly attributed to the nonlinearity of the atmosphere.

It is seen from the distributions of the contours of u and v in Fig. 7d and Fig. 8d that a very strong northeast flow is maintained over the Indian Ocean to West Pacific region of the Northern Hemisphere in July. Figure 7d shows that around 120°E to the north of equator, there is a weak jet of east wind, and to the south of equator, there is a strong jet of north wind. The prominent divergence of the northeast flow over this area leads to the maintenance of a strong divergence center in Fig. 7b near the equator and between 120°E and 160°E. However, it is seen from Fig. 7a that the intensive convective center is located around 10°N. The difference between the NCEP/NCAR reanalysis and the OLR-derived divergence may be attributed to the limitation of the capability of the model used in the reanalysis. Of course, the lack of observational data over this area is also an important cause for the difference.

From the above discussions, it is seen that in comparison with the earlier ECMWF and CAC analysis, the NCEP/NCAR reanalysis has made improvements in the description of the tropical divergent wind field. But for the Asian monsoon region, the problem in the descriptions with too strong intensity or bias in position of the divergent centers still exists. On the other hand, it is indicated from these results that in the tropics, although difficulties still exist for deriving precisely the atmospheric divergent wind from OLR data, it is feasible to use the OLR-derived divergent wind in the diagnostic studies of variations of the tropical atmospheric circulation, especially over the data-sparse oceanic areas. These tools can compensate, to some degree, the shortage of the observations in the tropical region.

V. APPLICATION OF OLR-DERIVED DIVERGENT WIND IN DIAGNOSTICS OF THE 1982–1983 ENSO EVENT

Numerous studies have shown that the anomalies in the tropical sea surface temperature (SST) may affect the vertical and horizontal atmospheric circulation and the climate at the low and middle latitudes. Until now, most of the results in the tropical circulation analyses are mainly based on the conventional observations with limited numbers of stations and tools (e. g., Teng and Fu 1990; Wang 1988; and Tourre et al. 1985). In this section, the Julian's scheme is used to calculate the monthly divergence field for the eight months (January, April, July and October, 1982 and 1983) over the tropical region within 35°N–35°S during 1982–1983 ENSO event. Then the divergent wind is decomposed meridionally and zonally for further calculating the indices of $I_w(\lambda)$ and $I_H(\varphi)$ and divergent wind components. Finally the maps of the Walker circulation and the Hadley circulation are derived month by month. In this section, our discussion will be concentrated on: 1) The new facts revealed from the OLR and comparing them with those from the conventional observations. 2) the anomalous circulation pattern in the tropics which is closely related to the anomalies of the climate in China.

Figure 9 shows the OLR-retrieved zonal circulation over the equatorial region (10°S–10°N) during the 1982–1983 ENSO event. The middle curve represents I_w . Shown in Fig. 9 is the evolution of the Walker circulation during the period of the 1982–1983 ENSO

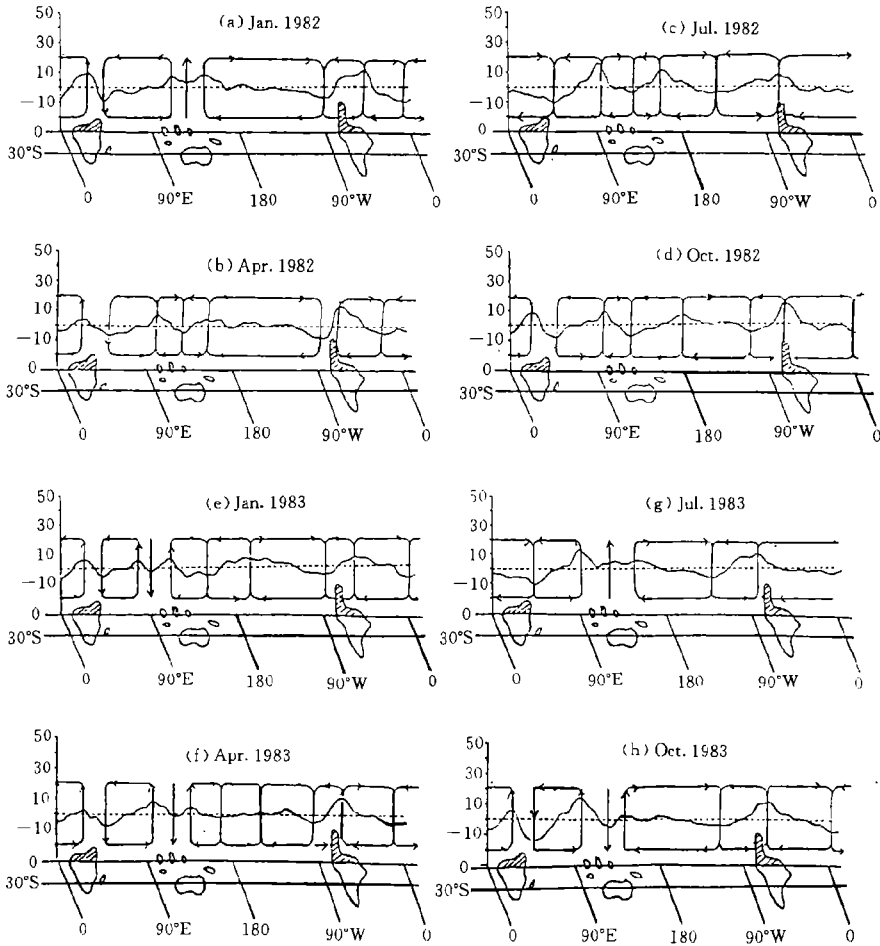


Fig. 9. The diagram of the equatorial Walker circulation during the 1982–1983 ENSO event, based on the mean U_z and $I_w(\lambda)$ along the equator (between 10°S–10°N) derived from the OLR data with J-scheme. The curves in the middle of diagram represent $I_w(\lambda)$ variation with longitude (λ).

event. To verify the reliability of the above-mentioned circulation, it is compared with those from other data sources. Figure 10a shows the Walker circulation calculated by Tourre et al. (1985) from the observational wind. Comparing Fig. 9e with Fig. 10a, there is a consistency concerning the ascending branch of the Walker circulation over the central-eastern Pacific and the descending branch over the Indian Ocean. But Fig. 9e displays much more details of the circulation. Comparing Fig. 9e with Fig. 10b which is obtained by Wang (1988) by using the surface observational wind, it is shown that there is a consistency between these two figures concerning the ascending branch over the central Pacific, the descending branch over the West Pacific, the ascending branch over Indian Ocean and the descending branch over the eastern Pacific. However, Fig. 9e also shows that there exists a weak ascending motion over the wide descending region of the eastern Indian to the West Pacific, which is absent in Fig. 10b. One possible reason is that

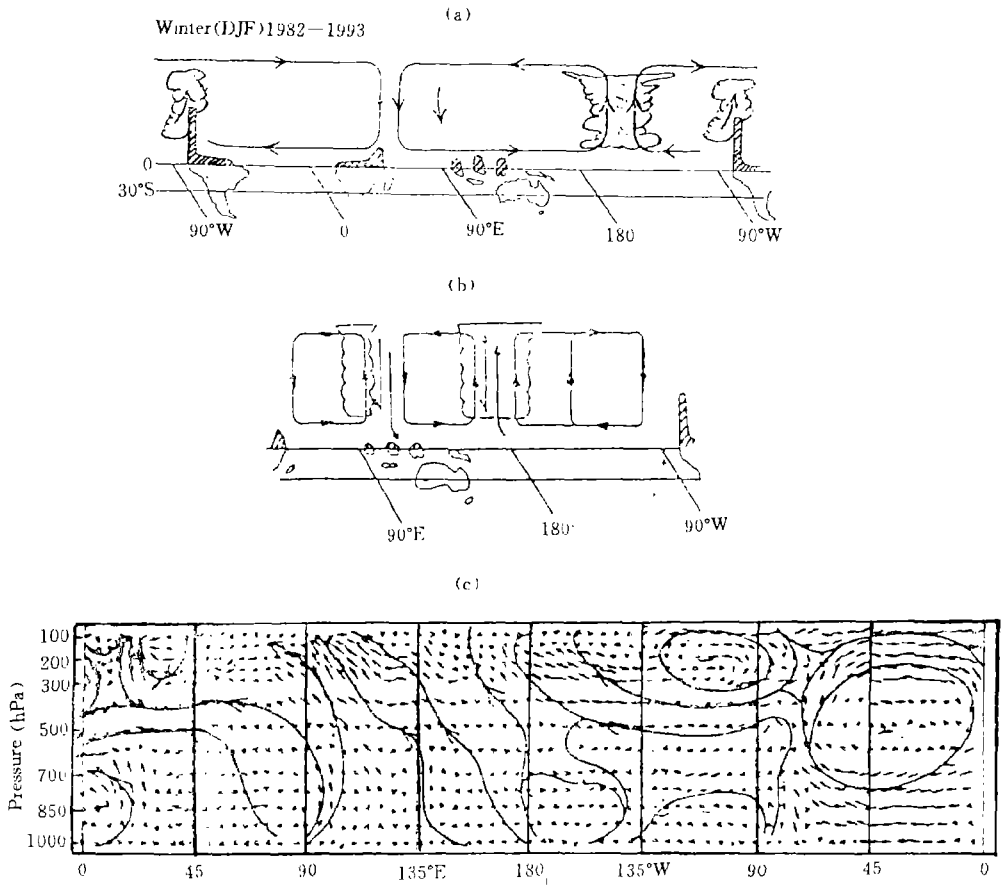


Fig. 10. (a) The diagram of the mean (between 30°S—30°N) Walker circulation for the 1982—1983 winter (DJF) given by Tourre et al. (1985); (b) The diagram of the Walker circulation during El Niño derived by Wang (1988) from observational wind; (c) The diagram of the Walker circulation of the December 1982 derived from ECMWF analysis by Teng and Fu (1990).

Fig. 10b represents the whole winter mean of several ENSO events and the data resolution ($10^{\circ} \times 10^{\circ}$) is much coarser than OLR data ($2.5^{\circ} \times 2.5^{\circ}$). Figure 10c shows the monthly mean Walker circulation in December 1982 given by Teng and Fu (1990) which is obtained from the wind of ECMWF analysis. It is shown that there exists no lower-level westerly and descending motion over the West Pacific, which is quite different from Figs. 10a, 10b and Fig. 9e. The limitation of the ECMWF analysis in the tropical divergent wind is shown again here.

An important phenomenon has been shown in Fig. 9 is that the development of the 1982—1983 ENSO event can not be described as a sudden reversal of the Walker circulation, but as the eastward movement of the ascending branch over the West Pacific from west to east along the equator during the development stage of the ENSO and passing through the date line during the peak stage in winter of 1982/1983. This leads significant

location shifts for the ascending and descending branches of Walker circulation. Meanwhile, the number of the ascending branches changes from 3 to 5 during the period from January 1982 through January 1983. It is worth noting that the two ascending branches over the South America and Africa are stable and stationary during the whole ENSO life cycle, but the ascending branches over the eastern Indian and the West Pacific are very unstable with splitting and moving eastward and finally passing through the date line, leading to the occurring of the ENSO. This fact raised some questions on how to explain theoretically the occurrence and development of the ENSO.

Now let us discuss the adjustment of the tropical Walker circulation and the West Pacific local Hadley circulation associated with climate anomalies in China in 1982–1983. It is indicated from Fig. 9 that the Walker circulation in the West Pacific displays large difference between 1982 and 1983. In January 1982, the ascending and descending motions dominated in the West Pacific and the central Pacific, respectively, while in January 1983, the descending and the ascending motions dominated in the West Pacific and the central Pacific, respectively. In July 1982, descending motion dominated in the West Pacific and the ascending motions dominated in the eastern Pacific, while in July 1983, the ascending motion dominated in the West Pacific, respectively.

It is obvious that such prominent variation of the tropical Walker circulation may affect the local Hadley circulation and further leads to the anomalies of climate in the middle latitudes. Figure 11 shows the variation of the local Hadley circulation in the West Pacific (110–160°E) during the winters and summers of 1982 and 1983. It is seen from Fig. 11 that the Hadley circulation is relative strong and its position is shifted to the north a little bit in January 1982, while the Hadley circulation weakened with its position more shifted to the south in January 1983. The local Hadley circulation weakened with its position shifted to the north in July 1982, while, the Hadley circulation became strong

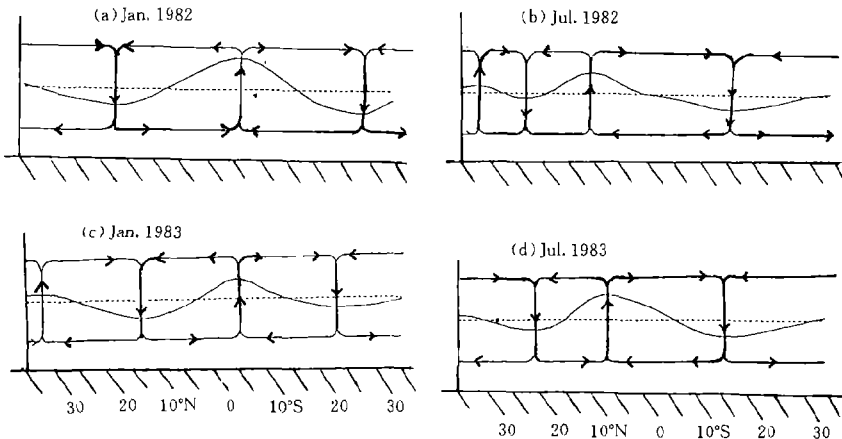


Fig. 11. The diagram of the local Hadley circulation over the West Pacific during 1982–1983 ENSO event, based on the mean (between 110–160°E) V_x and $I_H(\varphi)$ derived from OLR data with J-scheme. The curves in the middle represent the variation of $I_H(\varphi)$ with latitude.

with its position more shifted to the south in July 1983. The result is well in agreement with that of Jiang et al. (1989). Using the satellite data, they found that in the rainy years of the Changjiang River Valley, the ITCZ over the West Pacific was strong, more shifted to the south and the position of the subtropical high also shifted to the south.

Thus, from the above discussion it is clear that after the peak period of the ENSO event from winter 1982/1983 to summer 1983, the ascending branch of the Walker circulation re-maintained over West Pacific and enhanced the ascending motion strongly over there. Meanwhile, the local Hadley circulation over the West Pacific moved southward, its intensity was largely enhanced in the summer, with strong ascending motion over the region between $10^{\circ}\text{S} - 10^{\circ}\text{N}$. Consequently, it leads to the strong descending motion over South China and the north of the South China Sea. Further north, that is, the lower and middle reaches of the Changjiang River Valley, were under control of the ascending motion. Therefore, during the summer of 1983, the main rain belt was located there and the total rainfall was 20% to 100% higher than usual. At the same time, the drought occurred in South China and the number of landed typhoons was obviously reduced comparing to normal years (Fu 1987).

VI. CONCLUSIONS

Large number of calculation experiments and case studies show that it is practically feasible to estimate the tropical divergent wind by using the satellite-observed OLR data. The OLR derived divergent wind can compensate the lack of the observational wind data in low latitudes and correct the bias in the wind field analysis over the tropics. This method not only can be used to improve the initial divergent wind in the numerical weather prediction, but also can be used to diagnose the anomaly of the zonal and meridional circulation over the tropics. It is expected that this new tool will be used in the daily climate monitoring and diagnostic study in the near future.

The anomalies of the Walker circulation during 1982—1983 ENSO event consist in the progressive eastward movement and enhancement of its ascending branch over the West Pacific. The sharp changes of the local Hadley circulation over the central-eastern Pacific have close links with the variation of the ascending branches of Walker circulation. It implies the possible processes for the propagation of the anomalies from the tropics to the middle latitude in East Asian: the anomaly in tropical SST in the CEP can give rise to the anomaly of the Walker circulation and then bring forth the anomaly in the local Hadley circulation, finally leading to the climate anomaly in middle latitudes. Therefore, the further observational and theoretical clarification in the physical linkage between the anomalies of the Walker circulation and Hadley circulation will be helpful and valuable to further reveal the interaction between the low-latitude and mid-latitude processes and to enhance the predictability of the climate variability in mid-latitudes. The present paper involves only one ENSO case, further discussion is expected with more cases.

We would like to thank Prof. Xie An for his help in providing the program for converting the OLR to divergence in Julian's scheme and the anonymous reviewers for constructive suggestion. The OLR data used in this paper are provided by CAC.

REFERENCES

- Fu Congbin (1987). ENSO and interannual climate variability. *Chinese Journal of Atmospheric Sciences*, **11**: 209—220 (in Chinese).
- Jiang Shangcheng et al. (1989). The OLR characteristics in the flood and drought years of Changjiang River. *Acta Meteor. Sinica*, **47**: 494—498 (in Chinese).
- Jiang Shangcheng and Zhu Yafen (1990). *The OLR Atlas and Its Application*. Peking University Press. Beijing (in Chinese).
- Julian. P. R. (1984). Objective analysis in the tropics: A proposed scheme. *Mon. Wea. Rev.*, **112**: 1752—1767.
- Krishnamauti. T. N. (1986). On the relationship between the OLR and the divergent circulation. *J. Meteor. Soc. of Japan*, **64**: 709—719.
- Teng Xinlin and Fu Congbin (1990). A diagnostic analysis of winter atmospheric circulation during the 1982—1983 ENSO event. *Adv. Atmos. Sci.*, **7**: 57—66.
- Tourre et al. (1985). *Climate System Monitoring*. WCDP. WMO. p15.
- Wang Shaowu (1988). Walker circulation and meridional circulation in the equatorial Pacific. *Acta Oceanologica*, **7**: 56—64.
- Webster. P. J., Magana. V. O., Palmer. T. N., Shuklaa. J., Tomas. R. A., Yaanai. M. and Yasunari. T. (1998). The monsoon processes. predictability and the prospects for prediction. *J. Geophys. Res.*, **103** (C7), 14451—14510.
- Xie An and Bai Renhai (1993). Application of the satellite OLR data in the low latitudes wind field. *Acta Meteor. Sinica*, **51**: 218—226 (in Chinese).